Available online at www.sciencedirect.com
SCIENCE DIRECT
Surface Science 599 (2005) 14–26
SURFACE SCIENCE
www.elsevier.com/locate/susc

Preparation and characterization of well-ordered, thin niobia films on a metal substrate

D.E. Starr [a], F.M.T. Mendes [a,b], J. Middeke [c], R.-P. Blum [c], H. Niehus [c], D. Lahav [a], S. Guimond [a], A. Uhl [a], T. Kluener [a], M. Schmal [b], H. Kuhlenbeck [a], S. Shaikhutdinov [a,*], H.-J. Freund [a]

[a] *Department of Chemical Physics, Fritz-Haber Institut der Max-Planck Gesellschaft, Faradayweg 4-6, 14195 Berlin, Germany*
[b] *Federal University of Rio de Janeiro, NUCAT-PEQ-COPPE, Bl. G-128 Centro de Tecnologia, Cidade Universitária, Rio de Janeiro, Brazil*
[c] *Institut für Physik, Oberflächenphysik und Atomstossprozesse, Humboldt-University, Newtonstraße 15, 12489 Berlin, Germany*

Received 11 June 2005; accepted for publication 19 September 2005
Available online 27 October 2005

Abstract

Combining low energy electron diffraction, scanning tunneling microscopy, angular resolved photoelectron spectroscopy using synchrotron radiation and density functional theory calculations, we have studied the structure of thin niobia films grown on a $Cu_3Au(100)$ substrate. Nb deposition onto oxygen implanted $Cu_3Au(100)$ and subsequent oxidation results in a flat, well-ordered thin niobia film of hexagonal symmetry. The results suggest that the film consists of 2/3 ML of Nb between two hexagonal O-layers, where Nb^{5+} cations occupy the threefold hollow sites. This leads to a $(\sqrt{3} \times \sqrt{3})R30°$ structure with respect to the underlying close packed O layer, which in turn forms a (2×7) coincidence structure with the metal substrate. The defect structure includes reflection domain boundaries and vacancies.
© 2005 Elsevier B.V. All rights reserved.

Keywords: Thin oxide films; Epitaxy; Niobia; Scanning tunneling microscopy; Photoelectron spectroscopy; Density functional theory

1. Introduction

During the last two decades, niobia based systems have received much attention due to their catalytic activity in many important processes including Fischer–Tropsch reaction, oxidative dehydrogenation of alkanes, and oxidative coupling of methane ([1–5] and references therein). In

* Corresponding author. Tel.: +49 30 8413 4114; fax: +49 30 8413 4105.
E-mail address: shaikhutdinov@fhi-berlin.mpg.de (S. Shaikhutdinov).

0039-6028/$ - see front matter © 2005 Elsevier B.V. All rights reserved.
doi:10.1016/j.susc.2005.09.033

these catalysts, the niobium oxides can participate as either a support for metal particles or as an active component when added to other reducible oxides such as titania.

It is known that Nb forms several stable bulk oxides: NbO, NbO_2 and Nb_2O_5 [6]. The latter may exist in different polymorphs depending on its heat treatment [7–10]. The H–Nb_2O_5 phase exposes a Nb=O double bond, similar to vanadyl (V=O) species observed in vanadia based catalysts, the catalytic role of which remains a matter of the intense debate [4]. Therefore, comparisons of vanadia and niobia catalysts may be very helpful in revealing similarities and trends in reaction mechanisms on group V based metal oxide catalysts.

In attempts to understand the reactivity of oxide and metal/oxide surfaces, many research groups follow the "surface science" approach where the highly dispersed catalysts are modeled by metal particles vapor deposited onto well-ordered oxide films [11–13]. These systems allow one to elucidate mechanisms of the catalytic reactions on a molecular level through allowing precise structural control of the systems and their detailed analysis using the many surface sensitive techniques such as scanning tunneling microscopy (STM) and various electron spectroscopies. Within this approach, the preparation of well-ordered niobium oxide films is essential for modeling the structure of niobia based catalysts and providing a molecular level understanding of their reactivity.

In principle, thin oxide films may be prepared in different ways such as oxidation of metallic or bimetallic substrates, metal deposition onto an appropriate "inert" substrate and subsequent oxidation, or metal deposition in an oxygen atmosphere followed by further annealing at elevated temperatures (examples can be found in the reviews [13,14]).

The interaction of O_2 with Nb(1 0 0), Nb(1 1 0) and Nb(1 1 1) single crystal surfaces and Nb foils was the subject of several studies in the past and was recently re-investigated by STM [15–20]. Basically, these studies focused on the formation of a passivating film, which may strongly affect the superconducting properties of Nb. A number of oxygen induced reconstructions were observed by low energy electron diffraction (LEED) depending on the oxygen exposure and temperature. For example, An et al. [19] showed that increasing the exposure of Nb(1 0 0) to O_2 from 0.2 to 1.5 L ($1\ \mathrm{L} = 10^{-6}$ Torr s) at 300 K first produces a c(2 × 2)-O structure and then a (1 × 1)-O structure, but that further exposure to ~64 L results in an amorphous surface structure. Annealing at 900 K results in surface ordering into a (3 × 1)-O structure via the dissolution of oxygen into the bulk metal substrate. Due to the high solubility of oxygen in Nb, oxidized surfaces can also be formed by segregation of oxygen from the bulk to the surface upon heating to 1500–2500 K in vacuum. Using STM, Arfaoui et al. [17,18] observed NbO_x(1 1 1)-like nanocrystals (with $x = 0.8$–1.2), which form tiled structures on the Nb(1 1 0) surface with many stacking faults. These studies revealed that the Nb metal substrate may behave as an effective reservoir for oxygen, and hence cause uncertainty in the thickness and stoichiometry of the oxide film due to an ill-defined oxide/metal interface arising from difficulty in controlling oxygen diffusion.

Petrucci et al. applied molecular beam epitaxy to grow thick (100 Å–1.2 μm) niobia films on z-cut $LiNbO_3$, which were studied by reflection high energy electron diffraction (RHEED) [21]. Ex situ X-ray photoelectron spectroscopy (XPS) analysis of these films revealed Nb oxidation states of both 2+ and 5+, but after the films were further oxidized at 450 °C for 1 h in an oxygen atmosphere only Nb^{5+} was present. When grown on z-cut sapphire (Al_2O_3) at 650 °C at a low O_2/Nb flux ratio, the niobia films exhibited perfect RHEED reflections attributed to a well-ordered $NbO_{0.8}$(1 1 1) epitaxial layer, which could be converted to polycrystalline Nb_2O_5 by annealing at 420 °C for 3 h in a dry O_2 atmosphere.

Xie et al. [22,23] employed a Pt(1 1 1) single crystal as a substrate for the growth of niobia films using cycles of Nb deposition and oxidation. In each cycle, about 0.1 monolayer (ML) of Nb was evaporated onto the Pt(1 1 1) surface and then oxidized in 10^{-6}–10^{-5} mbar of O_2 at 700 K. Subsequently, the sample was annealed in ultra-high vacuum (UHV) at 800–900 K. At sub-monolayer Nb coverage (ca. 0.2 ML), LEED patterns (not presented in the paper) showed a hexagonal structure rotated by 30° with respect to Pt(1 1 1).

However, this pattern became very diffuse at increasing Nb coverage, suggesting that the niobia overlayer exhibited poor crystallinity. Based on the analysis of Auger electron spectroscopy (AES), high-resolution electron energy loss spectroscopy (HREELS) and ultraviolet photoelectron spectroscopy (UPS) data, the authors concluded that the thin films (ca. 3 ML) were composed of NbO, NbO_2 and Nb_2O_5, depending on the preparation conditions. A loss band at 926 cm^{-1} in HREELS spectra was assigned to Nb=O terminal bonds. However, the lack of ordering of the films prepared and the absence of any morphological studies renders the correlations between structure and spectroscopy speculative.

As a continuation of our long-term studies on the structure of the transition metal oxides [24,13], using well-defined model systems, we aimed at the preparation of well-ordered niobia films. It is well documented that oxide films of vanadium, neighboring Nb in the Periodic Table, can be prepared on the metal single crystal surfaces [25–28]. Further, it has recently been demonstrated that the quality of the vanadia films can be significantly improved when grown on a $Cu_3Au(100)$ substrate implanted with oxygen, which seems to prevent vanadium/substrate alloying and supplies atomic oxygen for oxidation [29,30]. In this paper, we used this approach to grow well-ordered niobia films and studied their structure by LEED, STM, photoelectron spectroscopy using synchrotron radiation (PES) and HREELS. The experimental results were complemented with density functional theory (DFT) calculations. The paper is organized as follows. We first present the experimental results obtained by each method for similarly prepared samples. This is followed by a summary of these results and a proposal for the structural model of the niobia films using DFT.

2. Experimental

The experiments were performed in three UHV chambers denoted as "STM", "PES" and "HREELS" (base pressure below 3×10^{-10} mbar). Each chamber was equipped with an AES/LEED, quartz crystal microbalance, differentially pumped mass-spectrometer and standard facilities for surface cleaning. The LEED patterns of the samples were used to judge the quality of the films for combining the results, obtained in different chambers.

The $Cu_3Au(100)$ single crystal (6 mm diameter and 2 mm thick) was supplied by Mateck. During the preparation, the temperature was controlled using a chromel–alumel thermocouple spot-welded to the edge of the crystal and a feedback control system (Schlichting Phys. Instrum). Heating was achieved by electron bombardment from the backside of the crystal using a W filament in "STM" and "PES" chambers. For the HREELS studies, the same $Cu_3Au(100)$ crystal was used, which was placed between two parallel Ta wires used for resistive heating.

The surface was cleaned by cycles of Ar^+ sputtering (1 keV, 2 $\mu A/cm^2$) at 300 K followed by annealing at 800 K for 5 min until no detectable impurities were found by AES. The traces of carbon, if any, were removed by oxidation at 600 K for 10–30 min at 10^{-6} mbar of O_2, followed by thermal flash to 800 K in UHV.

The clean $Cu_3Au(100)$ surface was sputtered at 300 K with oxygen, using the ion sputter gun (1 keV, 2×10^{-5} mbar of O_2, 30 min). Subsequently, the sample was annealed in vacuum at 650 K for 5 min to smooth the surface after sputtering. AES spectra from this surface showed O(510 eV)/Cu(948 eV) ratio of about 0.5. Niobium was vapor deposited onto the substrate kept at 300 K from a Nb rod (2 mm diameter, Goodfellow, 99.99%) using a commercial evaporator (Focus EFM3). The deposition rate was 0.04 Å/min as measured by a quartz crystal microbalance. Niobium was deposited in a single step in the amounts presented in the text as a nominal thickness (in Å). After Nb deposition, the samples were oxidized in 10^{-6} mbar O_2 at 773 K for 30 min in front of a calibrated gas doser.

The STM images were obtained with Pt–Ir tips at tunneling biases between +20 mV and +1.5 V (sample bias) and current 0.5–1 nA. The images presented here were subjected to plane corrections and low-pass filtering.

For PES studies we used synchrotron facilities at BESSY II (Berlin, beamline UE52-PGM1).

The spectra were taken with a Scienta SES200 analyzer. Spectra were recorded with photon energies of 121 eV (spectral resolution 100 meV), 310 and 830 eV (200–250 meV) for valence band, Nb 3d and O 1s levels, respectively. The energy was calibrated via the Fermi edge and also the binding energy of the Au 4f level of a clean gold foil and $Cu_3Au(100)$ substrate.

The HREELS spectra were measured with a Delta 0.5 spectrometer (VSI GmbH, a spectral resolution ~4 meV) in a specular geometry (grazing angle 30°) with a primary electron energy 5 eV.

DFT calculations were performed utilizing a commercial version of the CASTEP program available as a module of Cerius^2.[1] The system was simulated using a slab model containing three layers of $Cu_3Au(100)$, one layer of Nb and two layers of O stacked as O–Nb–O–Cu_3Au (3) in a (2×7) unit cell, using the PBE exchange-correlation functional [31] and ultrasoft non-local pseudopotentials [32]. A plane wave cutoff of $E_{cut} = 400$ eV was found to be sufficiently accurate. The surface Brillouin zone was sampled using eight special k-points.

3. Results

3.1. Low energy electron diffraction

Cu_3Au crystals have an L_{12}-structure with a lattice constant 3.75 Å and a shortest metal–metal distance of 2.65 Å. The surface structure of $Cu_3Au(100)$ is well documented in the literature [33]. Normal to the (100) surface, the Cu_3Au crystal consists of alternating pure Cu(100) and 1:1 [Au:Cu] layers in which two diagonal Cu atoms in the unit cell are substituted by gold. The LEED pattern of the clean $Cu_3Au(100)$ surface (not shown here for conciseness) thus exhibits diffraction spots similar to Cu(100) with the additional spots of a $c(2\times2)$ structure due to the presence of gold. The spots of this LEED pattern correspond to the distances of 3.75 Å and 2.65 Å along the {001} and {110} directions of the $Cu_3Au(100)$ surface. Utilizing these known distances and their corresponding directions allows us to calculate distances within the niobia film and its orientation with respect to the $Cu_3Au(100)$ surface.

Oxygen sputtering and annealing at 650 K produced no discernable changes in the LEED pattern. However, a previous study [34] has revealed that the oxygen implanted surface is enriched with Cu whereby oxygen occupies fourfold hollow sites, thus leading to the same $c(2\times2)$ LEED pattern as the clean, nontreated surface.

Deposition of Nb onto the O-implanted substrate in the sub-monolayer coverage regime and subsequent oxidation at 773 K results in LEED patterns as shown in Fig. 1. The intensities of the substrate spots gradually attenuate as the Nb coverage increases up to ~2 Å, which is consistent with niobia film growth via the formation and coalescence of two-dimensional niobia islands on the substrate.

The prevalent features in the LEED pattern presented in Fig. 1 are the three 12-spot rings clearly indicating the formation of an oxide layer with hexagonal symmetry. The presence of 12-spot rings can be readily attributed to two domains arising from two hexagonal mesh units rotated by 90° (or 30°) with respect to one another. The fact that the intensities of each spot within the rings are identical implies approximately equal coverages of the two domains on the surface. The three rings are distinguished from one another as one "inner" (1) and two "outer" rings (2, 3) as marked in Fig. 1a. The intensity of each ring depends on the electron energy; however the intensity of ring (2) always dominates the LEED pattern. Fig. 1b shows a schematic representation of the pattern where the spots from only a single domain are shown. Another domain is formed through rotation of this pattern by 90°.

For each domain, two of the six hexagonal spots of the ring (2) coincide with the (1×1) spots of the $Cu_3Au(100)$ substrate, indicating a good epitaxial relationship between the oxide film and the substrate. Such epitaxial growth has been previously reported for thin oxide films on metal substrates, such as NiO(111)/Ni(100) [35], VO(111)/Cu(100) [26], and FeO(111)/Pt(100) [36], i.e. for the films with a MO(111) stoichiometry.

[1] Cerius^2 is provided by Accelrys. Inc.

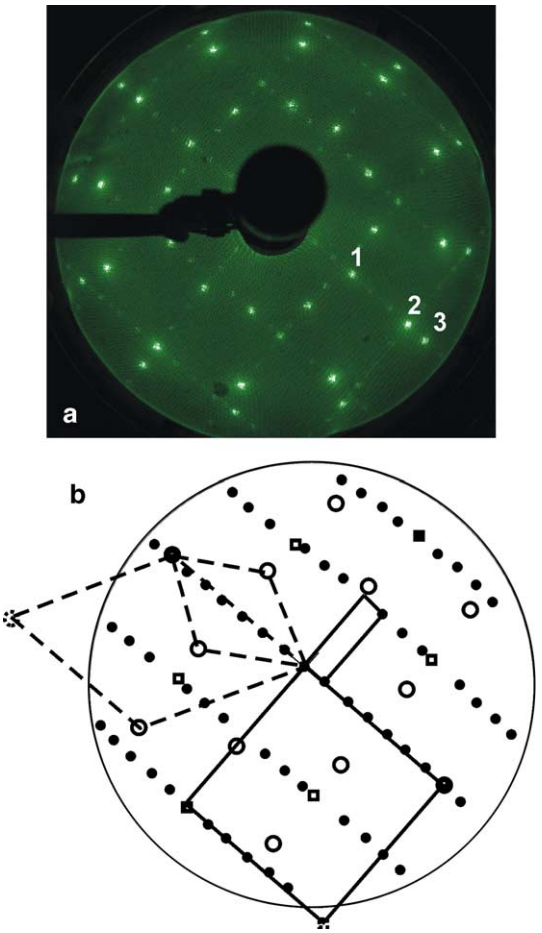

Fig. 1. (a) The LEED pattern ($E = 70$ eV) of the niobia film formed on $Cu_3Au(100)$–O by oxidation of a 1.6 Å-thick Nb layer at 773 K in 10^{-6} mbar of O_2. The 12-spot rings (1–3) are observed due to the presence of two hexagonal domains, rotated by 90°. (b) Schematic representation of the LEED pattern, where the spots from only a single domain are shown. Square symbols show spots from the $Cu_3Au(100)$ substrate. Open symbols are the most intense spots from the oxide film. Dots show the positions of weak spots due to a coincidence (2×7) structure. The surface unit cells of the substrate (solid square), the niobia film (dashed) and the coincidence structure (solid rectangle) are shown.

Therefore, we can assign the ring (2) to the O (or Nb) sub-lattice, which in real space can be expressed in matrix notation by

$$\begin{pmatrix} A' \\ B' \end{pmatrix} = \begin{pmatrix} 1 & -1/\sqrt{3} \\ 0 & 2/\sqrt{3} \end{pmatrix} \begin{pmatrix} A \\ B \end{pmatrix}$$

on the $Cu_3Au(100)$ surface. The vectors (A, B) indicate the unit vectors of the $Cu_3Au(100)$ substrate while the primed vectors are the unit vectors of the oxide sub-lattice. Using the known metal–metal distance on the $Cu_3Au(100)$ surface, we have calculated that the spots in ring (2) correspond to a distance of 3.1 Å, which is quite reasonable for O–O distance in oxide thin films. This then requires that the inner ring (1) is in a $(\sqrt{3} \times \sqrt{3})R30°$ registry with respect to the ring (2), with a characteristic distance of ~5.4 Å. Ring (3) is formed by the second order spots of ring (1).

In addition, the LEED pattern exhibits many diffraction spots, running along the $\{110\}$ and $\{\bar{1}10\}$ directions of the substrate. The intensity of these spots is weak, and they are most likely the result of the formation of a coincidence structure between the hexagonal overlayer and the square lattice of the $Cu_3Au(100)$ substrate. This coincidence structure has a (2×7) periodicity with respect to the $Cu_3Au(100)$ substrate corresponding to every sixth atom in the overlayer coinciding with every seventh metal atom on the substrate since 7×2.65 Å $= 18.55$ is almost equal to 6×3.1 Å $= 18.6$ Å. We also note that 2×2.65 Å $=$ 5.3 Å, which is close to the 5.4 Å distance calculated for the $(\sqrt{3} \times \sqrt{3})R30°$ structure.

In summary, LEED results show that the film contains at least one hexagonal layer, which forms a coincidence structure with respect to underlying metal substrate, and another layer(s) resulting in a $(\sqrt{3} \times \sqrt{3})R30°$ structure with respect to the hexagonal layer.

3.2. Scanning tunneling microscopy

Fig. 2a shows a large scale STM image of the thin niobia film covering the entire substrate displaying wide terraces separated by monatomic steps of the metal substrate underneath. No clusters or three-dimensional particles were observed. The image in Fig. 2b displays atomic protrusions forming a hexagonal lattice with a periodicity of ~5.5 Å agreeing well with the distance of 5.4 Å assigned to ring (1) in the LEED pattern of Fig. 1. The missing protrusions imaged as dark spots in Fig. 2b can be attributed to defects.

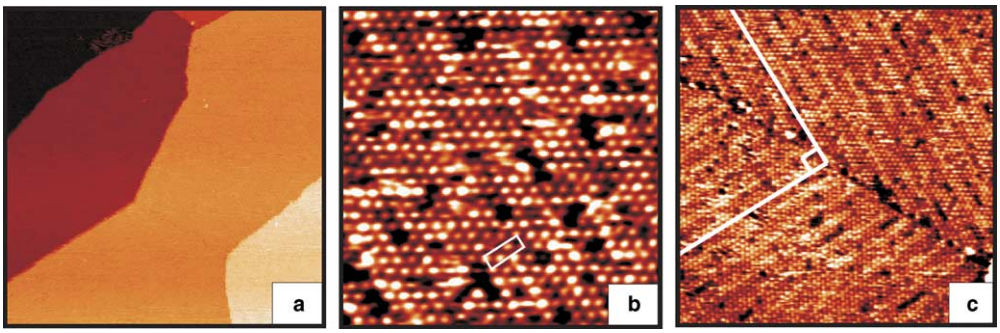

Fig. 2. STM images of the niobia film grown on $Cu_3Au(100)$. (a) Large terraces separated by steps of ~2 Å in height. (b) Hexagonal structure of the niobia film with vacancy defects. The (2×7) superstructure cell is marked as a rectangle. (c) Two domains rotated by 90°, with each domain exhibiting characteristic surface modulation seen as stripes. Image sizes and tunneling parameters are: (a) 200×200 nm^2, $V_S = 1.4$ V, $I = 1.0$ nA; (b) 15×15 nm^2, $V_S = 1.4$ V, $I = 1.0$ nA; (c) 40×40 nm^2, $V_S = 1.4$ V, $I = 1.0$ nA.

The terraces also exhibit a long-range modulation with a small (<0.2 Å) corrugation amplitude that is imaged as stripes in Fig. 2c. These stripes clearly reveal two domains rotated by 90° with respect to each other reflecting the square symmetry of the $Cu_3Au(100)$ substrate. These stripes run along the rows of protrusions and are four atomic rows wide, leading to a (1×4) superstructure with respect to the imaged protrusions. Note that, the same surface modulation is observed on niobia islands formed at sub-monolayer coverage, indicating that the film grows two-dimensionally.

Based on the height measurements of niobia islands formed at sub-monolayer Nb coverage, the thickness of the niobia film was measured to be ~2.5 Å. However, the apparent height measured by STM does not always represent the geometrical height due to the very different electronic structures of the oxide and metal substrates. Basically, the film thickness is underestimated due to a higher work function of the oxide surface than of the metal surface surrounding. Nonetheless, the results indicate that the thickness of the niobia film is indeed very small.

3.3. Photoelectron spectroscopy

In Fig. 3, photoelectron spectra are presented for two niobia films of different Nb coverage, which showed LEED patterns similar to that in Fig. 1. The spectra of the valence band (VB), the Cu 2p, O1s and Nb3d levels are shown at detection angles of both 0° and 70° with respect to the surface normal. Essentially the signals from the substrate elements attenuate upon film growth but no changes in the position and the widths of the peaks were observed. Based on these results, we conclude that no alloying or intermixing between the substrate and oxide film occurs.

The Nb 3d levels are spin–orbit split into two ($3d_{5/2}$ and $3d_{3/2}$) peaks. All binding energy (BE) values for the Nb 3d level discussed below refer to the position of the $3d_{5/2}$ peak. The Nb 3d signal, shown in Fig. 3 and exhibiting a peak centered at 206.4 eV, suggests the presence of a single Nb species in the film. In addition, the intensity of this peak does not depend on the detection angle indicating that the Nb species exist only in the surface region.

To date, most of the XPS data reported in the literature on Nb systems are analyzed based on the data presented in the review paper of Halbritter [37] summarizing the results obtained for the different Nb oxides. According to this review and also a recent paper of Morris et al. [38] on niobia powders, niobium in NbO_2 (Nb^{4+}) and Nb_2O_5 (Nb^{5+}) exhibits BE values of 205.8 and 207.5 eV, respectively. (To the best of our knowledge, there are no XPS studies on niobia single crystals). Therefore, the measured BE for our niobia films corresponds to oxidation state between 4+ as in NbO_2 and 5+ as in Nb_2O_5. However, for very thin oxide layers on metal substrates, the binding energies of the core electrons may in fact be lower than for thick oxide films and bulk systems due to the

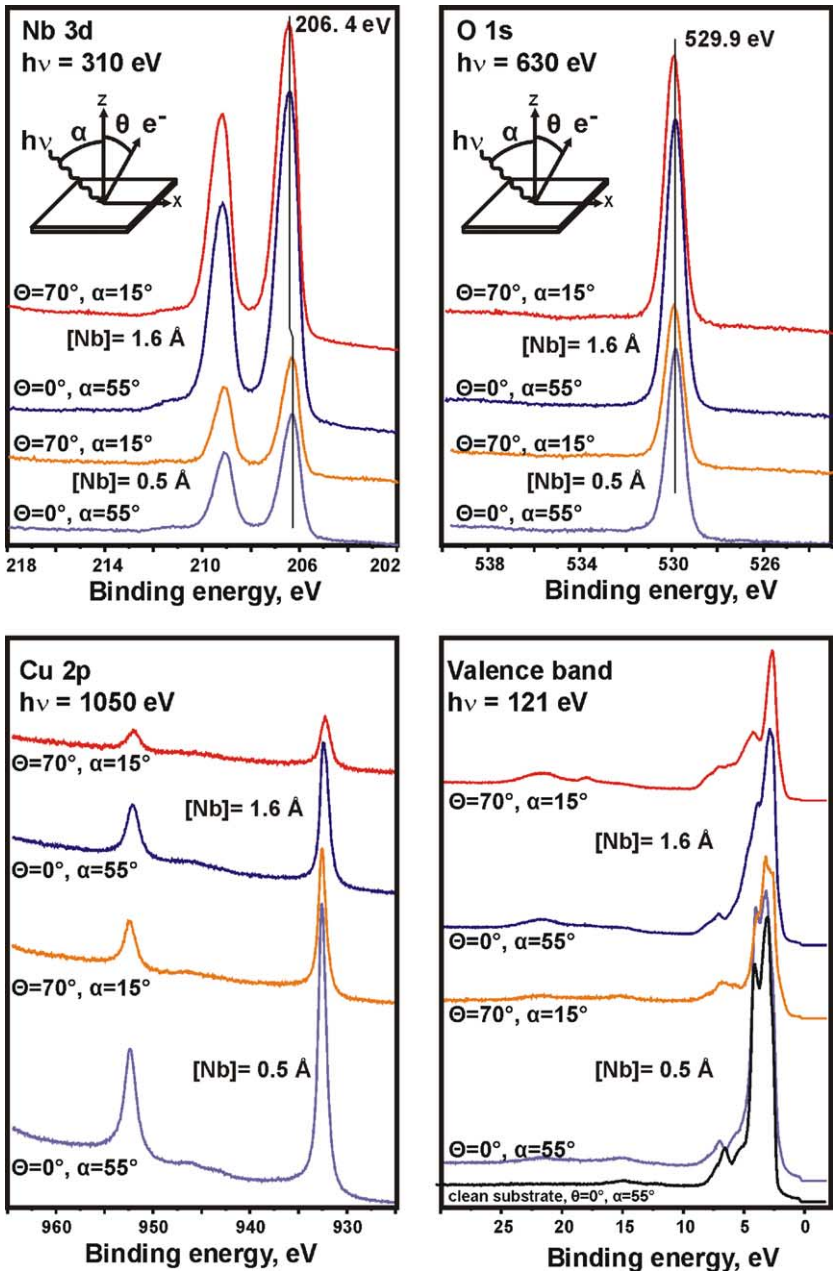

Fig. 3. Valence band, O 1s, Nb 3d, and Cu 2p photoelectron spectra of niobia films of 0.5 and 1.6 Å Nb coverage on $Cu_3Au(100)$. The angles between the surface normal and incident photon (α) and electron detector (θ) are indicated.

effective screening of the final state core hole by the metal substrate electrons.

The PE-spectra of oxygen do not help to clarify the situation. The BE of 529.9 eV for the O1s level in niobia films is close to those reported for many transition metal oxides. Although PES data for oxygen in niobium oxides are not available in the literature, we anticipate, similar to that observed

for vanadia systems [39], that the O1s level shifts only weakly as a function of the Nb oxidation state.

In principle, spectra of the VB region can provide a way to differentiate between Nb_2O_5 and NbO_2, as the first compound is an insulator with a band gap ~3.4 eV and the second is a semiconductor [38]. In NbO_2, since the metal is in a lower oxidation state, a feature near the Fermi edge emerges, which, in a simple ionic model, can be attributed to the *d*-electrons that have not been transferred to the oxygen anions and remain on the metal cations. The VB spectra of the bulk niobium oxides have been presented by Morris et al. [38]. In contrast to Nb_2O_5, the NbO_2 phase shows a well-resolved peak centered at 1.3 eV derived from the Nb 4d levels (NbO_2 is a $4d^1$ material) along with photoelectron intensity in the 4–10 eV range which is associated mainly with the O 2p levels. (Similar results have been also reported for $V_2O_5(0001)$ (insulator) and $V_2O_3(0001)$ (semiconductor) surfaces [40,41]).

The lack of intensity near the Fermi edge in the VB spectrum of our niobia films indicates that the film is non-conducting. There is no intensity at 1.3 eV as is observed for NbO_2, and also the 4–10 eV region does not resemble either the NbO_2 or Nb_2O_5 bulk valence band spectra. However, some intensity is observed near the onset of the substrate d-levels at ~2.5 eV. It seems quite plausible, that the valence band structure of the thin films of niobia is different from that of the bulk compounds.

Therefore, final state effects, leading to lower BE values, and the lack of intensity in the gap region of the VB spectra would seem to suggest Nb in our films in a fully oxidized 5+ state, which implies a Nb_2O_5 stoichiometry.

This conclusion is also consistent with quantitative analysis of the Nb and O signal ratio in AES spectra of the films (not shown here for conciseness). In order to avoid uncertainty caused by the different escape depths of electrons coming from different elements of the oxide film, we have used reference AES spectra of the MoO_3 and MoO_2 thin films [30]. Note also that the kinetic energies of the Auger electrons from metals are similar (cf. 168 eV for Nb and 186 eV for Mo). Using this approach, the results indicated a Nb:O elemental ratio in the films close to 1:2.5, i.e. a Nb_2O_5 stoichiometry.

4. Discussion

The LEED and STM results, presented above, clearly show the formation of a flat, well-ordered, thin niobia film on the $Cu_3Au(100)$ substrate. The oxide film grows two-dimensionally by forming niobia islands, which coalesce as the Nb coverage increases until the film covers the entire surface. This occurs at a coverage of approximately 0.7 ML of Nb with respect to the substrate lattice based on both STM and microbalance calibration of the Nb deposition flux. In addition, the film exhibits a two-domain structure, each rotated by 90° with respect to one another, reflecting the square symmetry of the $Cu_3Au(100)$ substrate. The STM and LEED results also indicate a hexagonal lattice with a 5.4 Å periodicity that is imaged as protrusions in STM. This distance agrees well with that measured by LEED for the spots in ring (1) (see Fig. 1), which form the $(\sqrt{3}\times\sqrt{3})R30°$ structure with respect to another hexagonal layer (ring 2) with a 3.1 Å lattice constant.

If we assign the 3.1 Å distance to a close-packed oxygen layer in contact with the metal substrate, the (2×7) superstructure observed in both LEED and STM is easily explained as the result of a coincidence structure between the hexagonal O sub-lattice and the square lattice of the substrate. Using the closest metal–metal distance of 2.65 Å on $Cu_3Au(100)$, which run in the {110} directions, and the relative orientations of the hexagonal oxygen lattice and the square substrate lattice, as observed in LEED, a superstructure can be created as shown in Fig. 4. In this structure, every sixth oxygen atom coincides with every seventh metal atom in the $\{\bar{1}10\}$ direction and every second metal atom in the {110} direction also coincides with an oxygen atom.

According to the PES and AES data a stoichiometry of our films is close to Nb_2O_5. If the niobia film only consisted of close-packed layers of O and Nb, this would result in a NbO(111) surface and no observation of a $(\sqrt{3}\times\sqrt{3})R30°$ structure in

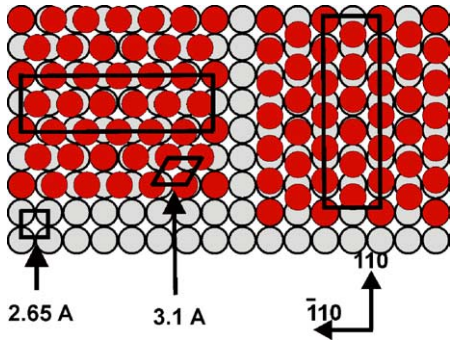

Fig. 4. Schematic representation of the (2×7) coincidence structure formed between the square lattice with $a_{110} = 2.65$ Å of the metal substrate and the hexagonal lattice with $a_{111} = 3.1$ Å of the oxide film. Two domains can be formed through rotation of the hexagonal lattice by 90° as indicated.

LEED. If we create this structure by removing 1/3 ML or 2/3 ML of Nb in $(\sqrt{3}\times\sqrt{3})R30°$ sites, it would lead to a Nb_2O_3 or NbO_3 stoichiometry, which is inconsistent with the PES results. Therefore, the model requires additional oxygen to be present beyond that of the close-packed O layer in contact with the substrate, stacked as O–Nb–O–(Cu_3Au). Within this stacking, creating a $(\sqrt{3}\times\sqrt{3})R30°$ structure by removing of 1/3 or 2/3 of the O atoms from any of the oxygen layers, while maintaining a close packed Nb layer, leads to a formal oxidation states below +2.5, which is also inconsistent with the experimental results. Therefore, the observation of a $(\sqrt{3}\times\sqrt{3})R30°$ structure must arise from the Nb sub-lattice rather than the O lattice.

In order to cover the entire surface, we have deposited approximately 0.7 ML of Nb as calibrated by quartz microbalance and STM. Therefore, a single $(\sqrt{3}\times\sqrt{3})R30°$ Nb layer (a coverage 0.33 ML), which would explain both the LEED and STM results, is not sufficient to account for the total Nb coverage. Alternatively, a layer of Nb, where 1/3 ML of Nb in $(\sqrt{3}\times\sqrt{3})R30°$ sites are missing, fulfills mass balance (the Nb coverage is 0.66 ML, i.e. close to the 0.7 ML) and maintains the unit cell observed in LEED. This is consistent with the PES results, indicating that Nb exists in a single oxidation state, and also explains the lack of angular dependence in the PES spectra (see Fig. 3).

Therefore, our results suggest that the film consists of 2/3 ML of Nb, which exhibits a $(\sqrt{3}\times\sqrt{3})R30°$ structure with respect to the close-packed O-layer and has another oxygen layer on top. Without the additional O layer, a Nb_2O_3 stoichiometry results that is inconsistent with the PES data. Such a "sandwich" structure is predicted to have a low net dipole moment normal to the surface, and hence be thermodynamically stable. However, if the top O-layer were identical to the bottom layer, this would lead to Nb in formal oxidation state 6+. In order to fit the Nb_2O_5 stoichiometry favored by the PES results, the top O-layer should possess 2/3 ML of oxygen.

In principle, the Nb atoms can occupy either threefold hollow or atop sites on the O-layer underneath and still maintain the same periodicity observed by LEED. In order to see, which adsorption sites are preferred, we have performed DFT calculations.

The substrate was included into a slab model containing three layers of $Cu_3Au(100)$ and one layer of Nb and two layers of O stacked as O–Nb–O–Cu_3Au (3) in a (2×7) unit cell. Fig. 5a shows four structures considered for the Nb_2O_5 films. These structures have been formed by constructing a top O-layer of the same structure as the Nb layer in order to maintain both the film unit periodicity observed by LEED and the Nb_2O_5 stoichiometry. These structures are formed through different registries of the oxygen and niobium layers such that the layer may sit either on top or on one of the two possible hollow (hcp and fcc) sites. Labeling the close-packed oxygen layer as A, the stacking of the layers for these structures may be termed AAA (top–top), ABB (fcc–top), ABC (fcc–hcp) and ABA (fcc–fcc) type stacking for structures 1, 2, 3 and 4 respectively.

Each structure was optimized within DFT, however, in order to reduce numerical efforts of calculations for the large unit cell, the first oxygen layer was fixed at a distance of 2 Å from the metal substrate, which is reasonable for the thin oxide films on metals [42,36]. The calculated total energies for the optimized geometry of the four structures shown in Fig. 5a indicate that structures 1 and 2 are the least stable. These structures are 6 eV and 2 eV less stable than the structure shown

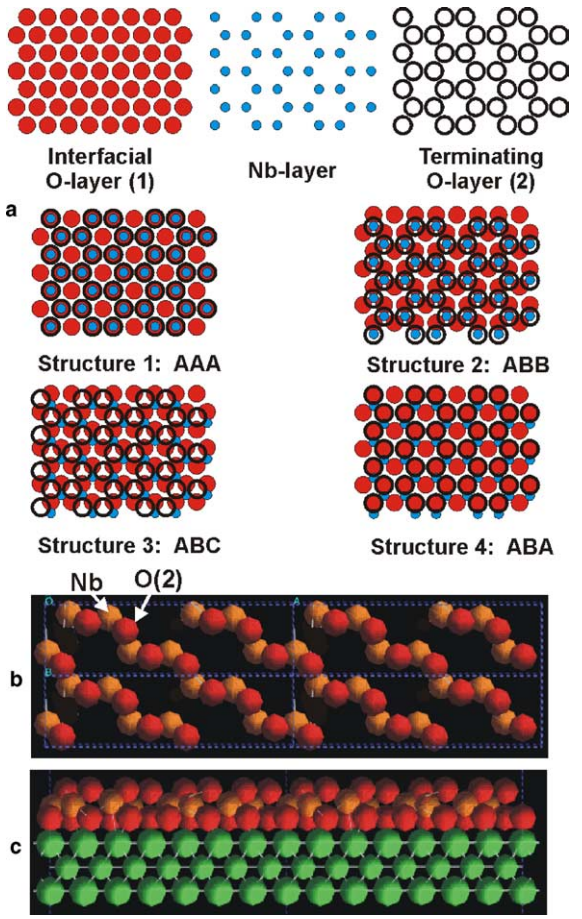

Fig. 5. (a) Four potential structures considered for the Nb_2O_5 film formed on $Cu_3Au(100)$ consistent with LEED and PES results. The structures are formed through different registries in the stacking sequences of the two oxygen and niobium layers shown in the top of the figure. In all structures the stacking sequence is O(2)–Nb–O(1)–(Cu_3Au); the metal substrate is not shown for clarity. The top (b) and side (c) views of the most stable structures determined by DFT. Only Nb and top O atoms are shown in the top view, for clarity.

in Fig. 5b, to which both structures 3 and 4 converge during DFT geometry optimization. This final structure is close to the structure 3 except that the oxygen atoms in the top layer have moved slightly out of the hollow sites towards Nb bridging sites. The fact that structures 1 and 2 did not converge to the lowest energy structure indicates the presence of local minima in the potential energy surface for these films and may be a result of fixing the position of the close-packed oxygen layer.

According to the DFT calculations the oxygen atoms do not prefer atop sites over Nb sub-lattice. Further evidence for this conclusion comes from HREELS measurements. If oxygen were sitting on top of the Nb atoms, one would expect the presence of niobyl (Nb=O) groups, which exhibit a characteristic absorption band in the 900–1000 cm^{-1} region of infrared and Raman spectra [43]. For example, niobia films grown on Pt(1 1 1) showed a strong signal at 926 cm^{-1} in HREELS which was assigned to niobyl groups [22,23]. For our thin films, the lack of any intensity in this region, as shown in Fig. 6, indicates that there are no niobyl species present on the film surface. According to the selection rules applied to HREELS of thin films on metal substrates, only the vibrations with the net dipole moment normal to the surface can be detected. Therefore, we have tentatively assigned the signal at 703 cm^{-1} as arising from O(2)–Nb–O(1) asymmetric vibrations, where O(2) and O(1) denote oxygen atoms in the top and bottom layers, respectively. (The small feature at 1406 cm^{-1} is the overtone of the 703 cm^{-1} peak). The weak shoulder located at ~870 cm^{-1} may be indicative of a small concentration of Nb=O stretching vibrations in distorted NbO_6 octahedra [43] and may lend insight into the structure of the defects present in our films.

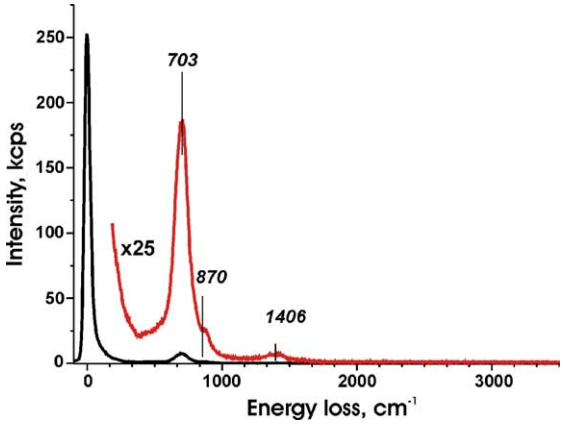

Fig. 6. HREELS spectrum for the thin niobia film grown on $Cu_3Au(100)$. The lack of significant intensity above ~900 cm^{-1} indicates the absence of niobyl groups (Nb=O) in our films.

For the most stable structure the DFT optimized geometry indicated interlayer distances of Nb–O(1), and O(2)–Nb to be ~1 and ~1.2 Å, respectively. Adding this to the 2 Å set for the O(1)–substrate distance, the film thickness would be around 4 Å, which is in qualitative agreement with the STM measurements (~2.5 Å).

Based on the calculated density of states, we have simulated STM images of the most stable structure at tunneling conditions used in the experiments based on the Tersoff–Hamann approach [44]. As shown in Fig. 7a, the simulated STM image matches well the experimental one and exhibits a hexagonal lattice of protrusions with a 5.4 A periodicity. The calculations showed that the STM protrusions on the surface are due to the unoccupied d-states of Nb and are located between two Nb atoms as seen in Fig. 7a. The charge difference plot shown in Fig. 7b revealed that there is no charge re-distribution and hence no direct interaction between these Nb atoms. Therefore, we have concluded that the protrusions observed in STM arise from pairs of "open" Nb atoms, which do not have a bridging oxygen atom above, which may screen these states.

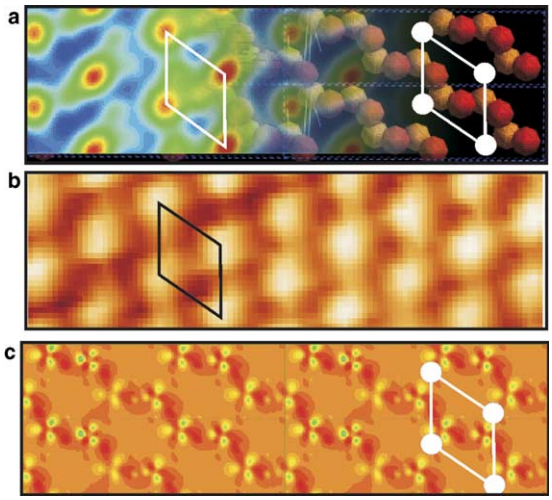

Fig. 7. Simulated (a) and experimental (b) STM images of the niobia film. The simulated image is superimposed with the positions of surface atoms in the model ($V_S = 1$ V, the tip-to-sample distance is set to 3 Å in the simulation). (c) The corresponding charge difference plot in the plane of the Nb layer. The positions of the STM protrusions over the surface are indicated by filled circles. The unit cell is indicated.

Interestingly, our structural model for the niobia film, which is consistent with all experimental results presented in this paper, is very similar to the model considered by Czekaj et al. [45] in their theoretical calculations of the $V_2O_3(0001)$ surface (model O_b^2VV' in their notation). The authors found this termination as the only one which could explain STM images of vanadia films grown on $Cu_3Au(100)$ [46]. On the other hand, numerous STM images for the films grown on Au(111), W(110), Pd(111) and Rh(111) (without oxygen implantation) are consistent with the presence of V=O groups experimentally proven on the same systems [27,28,40]. For the thin niobia films studied here and which were grown in a similar way as vanadia on $Cu_3Au(100)$, both theory and experiment rules out the presence of Nb=O species. Therefore, some discrepancy observed for differently prepared vanadia films may be associated with the exact preparation procedure. This issue will be further studied in combined STM and HREELS experiments of vanadia films on $Cu_3Au(100)$.

Finally, it is interesting to compare the structures of the thin niobia film to the structures of bulk Nb oxides. The film shows a hexagonal symmetry, with an O–O distance of 3.14 Å within the O-layer. This distance is only 5% larger than 2.98 Å for NbO(111) [6], but the latter structure must be excluded, based on the PES results. In principle, the (001) plane of the oxides with the rutile structure like TiO_2 or MoO_2 can also result in a close packed oxygen layer with the distances of about 3 Å, but the cations exposed on these surfaces form a rectangular and not a hexagonal lattice as observed here for the niobia films. Among various Nb_2O_5 polymorphs, only a TT-phase shows a pseudo-hexagonal lattice in the (*ab*) plane [47]. However, the Nb–Nb distance within this plane leads to a periodicity of 3.53 Å, which does not fit a 5.4 Å periodicity as well as the closest Nb–Nb (O–O) distance of 3.1 Å observed in this thin film. We have also inspected other cuts of the TT-Nb_2O_5 crystal structure, but none of them appear to fit the distances measured in our niobia film. Therefore, we can conclude that the surface of the thin niobia film in our study does not bear any periodicities similar to the surfaces of bulk niobium oxides formed by simple bulk truncation. However,

this does not preclude that truncating a bulk structure does not lead to reconstructions in the surface region resulting in surface structures with periodicities differing from those within the bulk.

5. Summary

We have grown thin niobia films on an oxygen implanted $Cu_3Au(100)$ substrate by Nb deposition and subsequent oxidation at 773 K in 10^{-6} mbar of O_2. The surface structure of the films has been studied using LEED, STM, HREELS and angular resolved PES.

The oxide film grows two-dimensionally by forming niobia islands, which coalescence at increasing Nb coverage. The film covers the entire substrate at the coverage equivalent to about 0.7 ML of Nb. The film exhibits a hexagonal symmetry with a lattice constant of 5.4 Å. The results suggest that the film consists of 2/3 ML of Nb between two hexagonal O-layers, where Nb^{5+} cations occupy the threefold hollow sites. This leads to a $(\sqrt{3} \times \sqrt{3})R30^\circ$ structure with respect to the underlying close packed O layer, which in turn forms a (2×7) coincidence structure with the metal substrate. The defect structure includes reflection domain boundaries and vacancies.

Comparison of the film structure with those known for bulk niobia leads to the conclusion, that the surface of thin niobia film does not resemble any of those structures if the latter do not reconstruct. However, it well may be that "monolayer" niobia catalysts supported at low loading on other oxide supports such as Al_2O_3, TiO_2, etc. also show structures different from the bulk. Despite vast amounts of research efforts, the molecular structure of the supported niobium oxide catalysts is not well understood and may be quite different from the structures formed through simple bulk truncation as observed in this work.

Acknowledgements

We acknowledge support of the Deutsche Forschung Gemeinschaft through SFB 546. F.M.T. Mendes and M. Schmal acknowledge the financial support from Coordenação de Aperfeiçoamento de Pessoal de Nível Superior, CAPES-Brasil (Grant—BEX2454/03-3). We also thank A. Doyle and M. Abu Al-Haija for technical support.

References

[1] J.-M. Jehng, I.E. Wachs, Catal. Today 8 (1990) 37.
[2] M. Ziolek, Catal. Today 78 (2003) 47.
[3] K. Tanabe, Catal. Today 78 (2003) 65.
[4] I.E. Wachs, Catal. Today 100 (2005) 79.
[5] F.M.T. Mendes, F.B. Noronha, M. Schmal, Stud. Surf. Sci. Catal. 130 (2001) 3717.
[6] R.W.G. Wyckoff, Crystal Structures, second ed., Wiley, New York, 1963.
[7] B.M. Gatehouse, A.D. Wadsley, Acta. Cryst. 17 (1964) 1545.
[8] H. Schafer, R. Gruehn, F. Schulte, Angew. Chem. Int. Ed. 5 (1966) 40.
[9] V.K. Kato, S. Tamura, Acta. Cryst. B 31 (1975) 673.
[10] J.G. Weissman, E.I. Ko, P. Wynblatt, J.M. Howe, Chem. Mater. 1 (1989) 187.
[11] C.T. Campbell, Surf. Sci. Rep. 27 (1997) 1.
[12] D.R. Rainer, D.W. Goodman, J. Mol. Catal. A 131 (1998) 259.
[13] M. Bäumer, H.-J. Freund, Prog. Surf. Sci. 61 (1999) 127.
[14] S.C. Street, D.W. Goodman, Ann. Rev. Phys. Chem. 48 (1997) 37.
[15] H.H. Farrell, M. Strongin, Surf. Sci. 38 (1973) 18.
[16] A. Darlinski, J. Halbritter, J. Vac. Sci. Technol. A 5 (1987) 1235.
[17] I. Arfaoui, J. Cousty, H. Safa, Phys. Rev. B 65 (2002) 115413.
[18] I. Arfaoui, J. Cousty, C. Guillot, Surf. Sci. 557 (2004) 119.
[19] B. An, S. Fukuyama, K. Yokogawa, M. Yoshimura, Phys. Rev. B 68 (2003) 115423.
[20] C. Sügers, M. Schöck, H. van Löhneysen, Surf. Sci. 471 (2001) 209.
[21] M. Petrucci, C.W. Pitt, S.R. Reynolds, H.J. Milledge, M.J. Mendelssohn, C. Dineen, W.G. Freeman, J. Appl. Phys. 63 (1998) 900.
[22] L. Xie, D. Wang, C. Zhong, X. Guo, T. Ushikubo, K. Wada, Surf. Sci. 320 (1994) 62.
[23] T. Ushikubo, Y. Koike, K. Wada, L. Xie, D. Wang, X. Guo, Catal. Today 28 (1996) 59.
[24] H.-J. Freund, Angew. Chem. Int. Ed. 36 (1997) 452.
[25] K.B. Lewis, S.T. Oyama, G. Somorjai, Surf. Sci. 233 (1990) 75.
[26] K. Kishi, Y. Hayakawa, K. Fujiwara, Surf. Sci. 356 (1996) 171.
[27] S. Surnev, M.G. Ramsey, F.P. Netzer, Progr. Surf. Sci. 73 (2003) 117.
[28] A.-C. Dupuis, M. Abu Al-Haija, B. Richter, H. Kuhlenbeck, H.-J. Freund, Surf. Sci. 539 (2003) 99.

[29] H. Niehus, R.-P. Blum, D. Ahlbehrendt, Phys. Status Solidii (a) 187 (2001) 151.
[30] J. Middeke, R.-P. Blum, H. Niehus, Surf. Sci. 587 (2005) 219.
[31] J.P. Perdew, K. Burke, M. Ernzerhof, Phys. Rev. Lett. 77 (1994) 3865.
[32] D. Vanderbilt, Phys. Rev. B 41 (1990) 7892.
[33] T.M. Buck, G.H. Wheatley, L. Marchut, Phys. Rev. Lett. 51 (1983) 43.
[34] H. Niehus, C. Achete, Surf. Sci. 289 (1993) 19.
[35] O.L. Warren, P.A. Thiel, J. Chem. Phys. 100 (1994) 659.
[36] Sh. Shaikhutdinov, M. Ritter, W. Weiss, Phys. Rev. B 62 (2000) 7535.
[37] J. Halbritter, Appl. Phys. A 43 (1987) 1.
[38] D. Morris, Y. Dou, J. Rebane, C.E.J. Mitchell, R.G. Egdell, D.S.L. Law, A. Vittadini, M. Casarin, Phys. Rev. B 61 (2000) 13445.
[39] J. Mendialdua, R. Casanova, Y. Barbaux, J. Electr. Spectr. Relat. Phenom. 71 (1995) 249.
[40] J. Schoiswohl, M. Sock, S. Surnev, M.G. Ramsey, F.P. Netzer, G. Kresse, J.N. Andersen, Surf. Sci. 555 (2004) 101.
[41] W. Xiao, K. Xie, Q. Guo, E.G. Wang, J. Phys. Chem. B 106 (2002) 4721.
[42] J. Schoiswohl, M. Sock, S. Eck, S. Surnev, M.G. Ramsey, F.P. Netzer, G. Kresse, Phys. Rev. B 69 (2004) 155403.
[43] J.-M. Jehng, I.E. Wachs, J. Phys. Chem. 95 (1991) 7373.
[44] J. Tersoff, D.R. Hamann, Phys. Rev. B 31 (1985) 805.
[45] I. Czekaj, K. Hermann, M. Witko, Surf. Sci. 545 (2003) 85.
[46] H. Niehus, R.-P. Blum, D. Ahlbehrendt, Surf. Rev. Lett. 10 (2003) 353.
[47] L.A. Aleshina, V.P. Malinenko, A.D. Phouphanov, N.M. Jakovleva, J. Non-Crystal. Sol. 87 (1986) 350.